Impact Factor:					
	ISRA (India) = 6.317	SIS (USA) = 0.912	ICV (Poland) = 6.630
	ISI (Dubai, UAE) = 1.582	РИНЦ (Russia) = 3.939	PIF (India) = 1.940
	GIF (Australia) = 0.564	ESJI (KZ) = 8.771	IBI (India) = 4.260
	JIF = 1.500	SJIF (Morocco) = 7.184	OAJI (USA) = 0.350

SOI: 1.1/TAS DOI: 10.15863/TAS

International Scientific Journal

Theoretical & Applied Science

p-ISSN: 2308-4944 (print) **e-ISSN:** 2409-0085 (online)

Year: 2022 **Issue:** 04 **Volume:** 108

Published: 22.04.2022 **http://T-Science.org**

Issue Article

Akhror Abdukholisov
National University of Uzbekistan
Republic of Uzbekistan, Tashkent, University str.,
akoshji@gmail.com

Alisher Gulumbaevich Eshimbetov
Institute of Bioorganic Chemistry
Senior scientist of the laboratory of Complex compounds,
Uzbekistan Academy of Sciences Republic of Uzbekistan, Tashkent, Mirzo Ulugbek str.,83.
ealisherg@yahoo.com

Surayyo Razzoqova
National University of Uzbekistan
Republic of Uzbekistan, Tashkent, University str.,
razzakova89@mail.ru

Jamshid Mingnorovich Ashurov
Institute of Bioorganic Chemistry
Senior scientist of the laboratory of Complex compounds
Uzbekistan Academy of Sciences Republic of Uzbekistan,
Tashkent, Mirzo Ulugbek str., 83
atom.uz@mail.ru

DFT STUDY OF THE SOLVATE OF α-(N-BENZOXAZOLINE-2-ONE) ACETIC ACID WITH FORMIC ACID COMPARING TO ITS COMPOSITION PARTS

Abstract: *Present work describes the DFT studies of α-(N-Benzoxazolin-2-one)acetic acid and its solvate with formic acid comparing to N-benzoxazoline-2-one and 2-aminoacetic acid. The electronic structures of these compounds are considered using quantum chemical parameters, the distribution of the total charge and the surface of the electrostatic potential on the atoms. In addition, non-covalent interactions were studied for the solvate molecule.*

Key words: *benzoxazolin-2-one, α-(N-Benzoxazolin-2-one)acetic acid, DFT, ESP surface, global quantum-chemical parameters.*

Language: *English*

Citation: Abdukholisov, A., Eshimbetov, A. G., Razzoqova, S., & Ashurov, J. M. (2022). DFT study of the solvate of α-(N-benzoxazoline-2-one) acetic acid with formic acid comparing to its composition parts. *ISJ Theoretical & Applied Science, 04 (108)*, 549-553.

Soi: http://s-o-i.org/1.1/TAS-04-108-64 ***Doi***: crossref https://dx.doi.org/10.15863/TAS.2022.04.108.64

Scopus ASCC: *1600.*

Introduction

Benzoxazolin-2-one and some of its derivatives are important chemicals as fungicides against crop diseases [1-3]. Therefore, a large amount of literature [4, 5] is devoted to the synthesis of new derivatives of benzoxazolone-2 and their testing against various types of diseases of cultural plants. Additionally, the structure were studied by XRD methods and theoretical methods [6-10] in a number of works. The presence of labile proton on the carboxyl group of α-

(*N*-Benzoxazolin-2-one) acetic acid. α-(N-Benzoxazolin-2-one) acetic acid can participate in intermolecular interactions through the labile proton of the carboxyl group and it can be easily deprotonated. Due to this proton, a solvate of α-(N-Benzoxazolin-2-one)acetic acid with formic acid was obtained [7].

Theoretical analysis of the solvate using quantum chemical parameters in comparison with its constituents makes it possible to reveal changes in the electronic structure of the solvate and α-(N-benzoxazolin-2-one) acetic acid. In this regard, we studied the electronic structure of α-(N-benzoxazolin-2-one) acetic acid and its solvate with formic acid in comparison with N-benzoxazolin-2-one and 2-aminoacetic acid by DFT method.

Materials and methods

The objects of our study are α-(*N*-Benzoxazolin-2-one)acetic acid (BAA) and its solvate with formic acid – solvate of α-(*N*-Benzoxazolin-2-one)acetic acid – SBAA. Besides, 2-Benzoxazolinone (BO) and 2-aminoacetic acid (AA) also were considered as composition part of α-(*N*-Benzoxazolin-2-one) acetic acid.

The synthesis of the SBAA was described early and identified by single crystal XRD method [7]. The initial geometry of BAA and SBAA were taken from XRD data (.cif files).

The calculations have been carried out by large basis set 6-311++G(d,p) including polarization and diffusion functions for H atom and heavy atoms, which successfully used in early work [8].

All calculations have been performed using ORCA 5.0 [11] program package. The results of calculations are visualized by Avogadro [12] software. The electrostatic potential surface were calculated by MultiWFN [13] program and it is analyzed by VMD [14] program.

Results and discussion

The geometries of studied compounds have been fully optimized by B3LYP/6-311++G(d,p).

Then optimized structured were correlated with XRD geometries of BAA and SBAA (Table 1). The obtained satisfactory correlations show the possibility of using this method to calculate other characteristics of the studied compounds.

Table 1. The comparison of XRD and theoretical bond lengths (angles)

Compound	MAE, Å (°)	LE, Å (°)	R^2
BAA	0.01 (0.84)	0.034 (2.6)	0.95 (0.97)
SBAA	0.92 (0.94)	1.88 (3.9)	0.95 (0.97)

The Mulliken analysis of the charge distribution on the atoms of compounds BAA and SBAA shows a significant change in the charge on the C4 and N3 atoms comparing to its composition parts (AA, BA). These changes can be explained by the inductive (-I) effect of acetic acid in the case of BAA and SBAA (Fig.1).

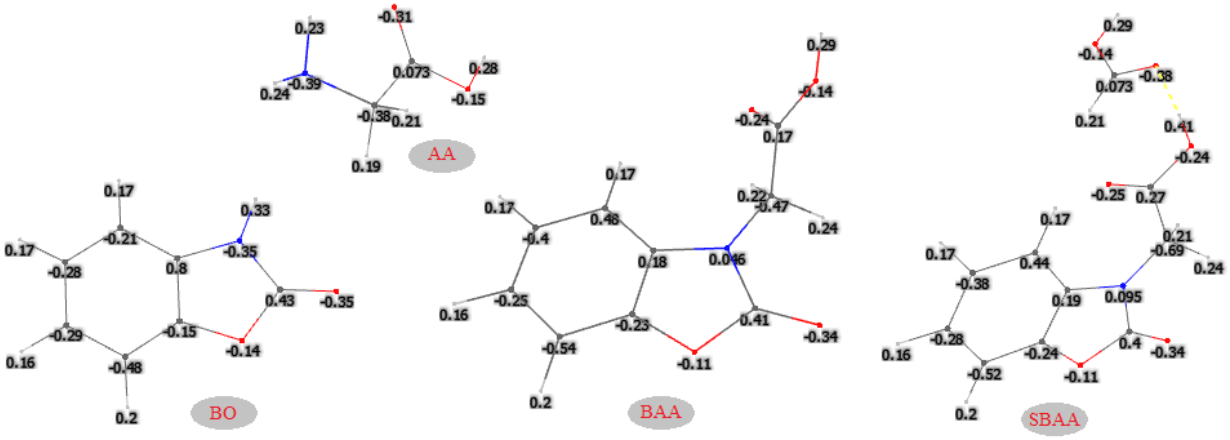

Fig.1. Charge distribution on the atoms of the 2-AA, BO, BAA and SBAA.

It is known that HOMO and LUMO play a huge role in chemistry and pharmaceuticals, since many reactions and biological processes (binding of a ligand to a receptor) can be proceed with the participation of these orbitals [15-16]. The electron densities on HOMO and LUMO of BA, BAA and SBAA are illustrated in figure 2. Similar pictures of HOMO and LUMO for BA and BAA have been found, which is localized in the 2-benzoxazolinone ring. However, in the case of solvate (SBAA) the LUMO is localized in

formic acid part of the cocrystal. In a number of BA, BAA and SBAA, the level of HOMO increases and the energy gap decreases. In the solvate, the system is stabilized by intermolecular hydrogen bonding with the participation of the BAA carboxyl group and carbonyl oxygen and the hydrogen atom of formic acid. This is reflected in the energy gap of the solvate (Table 2). In table 2, the global quantum-chemical parameters [17-18] are determined based on HOMO and LUMO energies of BA, BAA and SBAA.

Table-2. Quantum-chemical parameters for BA, 2-AA, BAA and SBAA

Quantum-chemical parameters	BA	BAA	SBAA
E_{HOMO} (eV)	-6.50	-6.44	-6.32
E_{LUMO} (eV)	-0.91	-0.87	-1.19
Energy gap, $\|\Delta E\| = E_{HOMO} - E_{LUMO}$ (eV)	5.59	5.57	5.13
Ionization Potential, $I = - E_{HOMO}$ (eV)	6.50	6.44	6.32
Electron Affinity, $A = - E_{LUMO}$ (eV)	0.91	0.87	1.19
Electronegativity, $\chi = (I + A)/2$ (eV)	3.70	3.65	3.75
Chemical hardness, $\eta = (I - A)/2$ (eV)	2.79	2.78	2.56
Chemical potential, $\mu_p = - (I + A)/2$ (eV)	-3.70	-3.65	-3.75
Chemical softness, $\sigma = 1/(2\eta)$ (eV^{-1})	0.18	0.18	0.19
Electrophilicity index, $\omega = \mu_p^2/2\eta$ (eV)	2.46	2.4	2.75

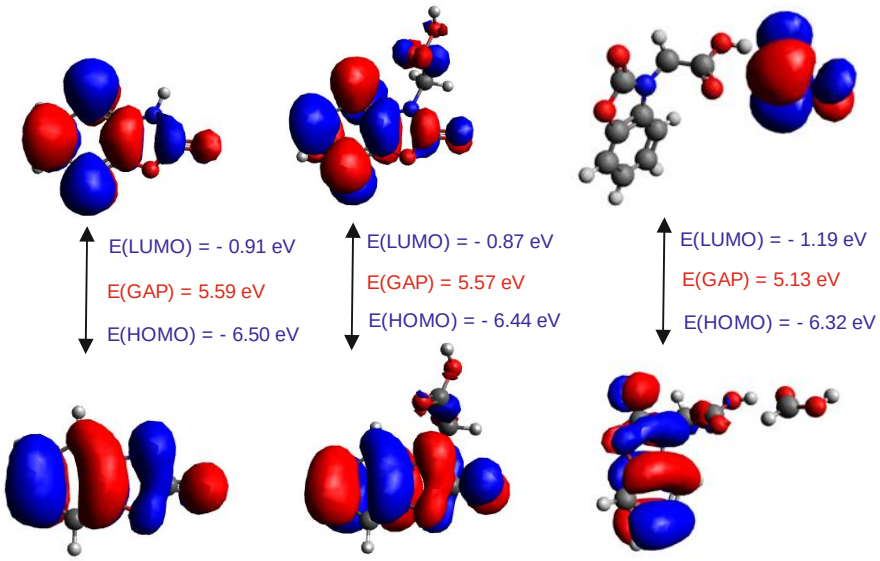

Fig.2. Electron densities on HOMO (left) and LUMO (right)

The electrostatic potential (ESP) surface analysis is powerful parameter that describes electron-rich and electron-deficit centers of molecule [19]. The ESP surfaces of BAA and SBAA are demonstrated in Fig. 3. In the ESP surface, red parts (positive numbers) are maxima and they indicate electron-deficit centers, which prone to attack by nucleophiles. Blue parts (negative numbers) are minima and these centers are rich in electrons. The maximum (57.10 kcal/mole) is located on vicinity of the H atom of the COOH group in the case of BAA. However, in the case of SBAA, the maximum is localized near to the H atom (61.52 kcal/mole) of the COOH group of formic acid. The minima are situated in near to oxygen atoms of the benzoxazolin-2-one ring and C=O group. It should be pointed that the smallest minimum is found near the oxygen atom of >C=O (-39.11 kcal/mole) group. The next smallest minimum falls on the oxygen atom of the COOH group (-29.16 kcal/mole). The last smallest minimum is located on vicinity of the oxygen atom of the oxazole ring (-25.81 kcal/mole).

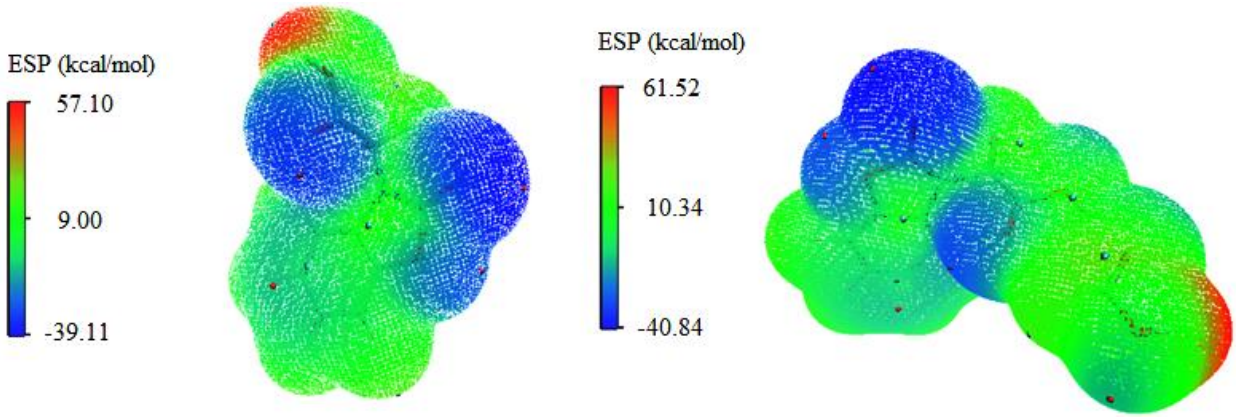

Fig.3. ESP surface maxima and minima for BAA and SBAA

In Fig.4, non-covalent interactions (NCI) and RDG plot [20-23] are given for visualization of specific interactions in solvate (SBAA). The RDG isosurface map is illustrated as reduced density gradients (RDG, Y axes) versus electron density multiplied by the sign of the second Hessian eigenvalue (X axes). The $(\lambda_2)\rho$ sign values indicate the strength of the interaction, attractive interactions have large negative $(\lambda_2)\rho$ sign values, while steric effects have large positive $(\lambda_2)\rho$ sign values. The regions of weak Van der Waals interaction have sign values $(\lambda_2)\rho$ close to zero [23].

The presence of strong H-bond (attractive force) is highlighted in blue color. The strong repulsive force (steric effect) is indicated in red color. Weak interactions (Van der Waals interactions) are highlighted with a green color [20-23].

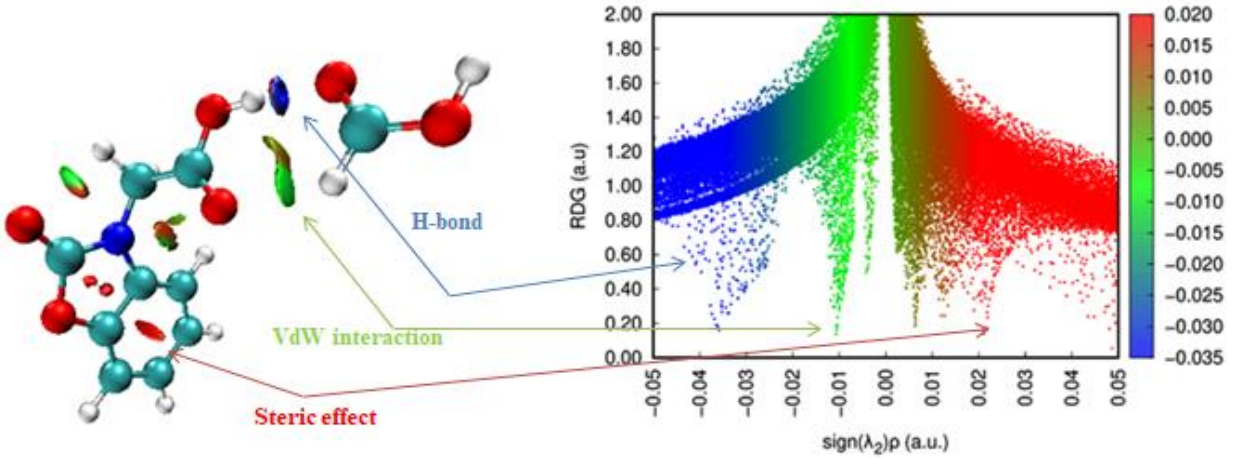

Fig.4. NCI and color-filled RDG map for SBAA

Conclusion

Thus, the electronic structure of compound 1 and its constituents was studied. The Mulliken analysis of the charge distribution on the atoms of compounds BAA and SBAA shows a significant change due to the inductive (-I) effect of acetic acid in the charge on the C4 and N3 atoms comparing to its composition parts (AA, BA). In the case of solvate, a significant change is occurred in O and H atoms of COOH group of α-(N-Benzoxazolin-2-one) acetic acid. In the case of solvate, an electron density in HOMO is localized in the ring of 2-benzoxazolinone and LUMO is localized in formic acid. This shows that in orbital-controlled processes, α-(N-Benzoxazolin-2-one) acetic acid can enter as an electron donor particle. The presence of strong H-bond, steric effect and VdW-interactions visualized by Non-covalent interactions and color-filled RDG plots.

References:

1. Balaswamy, G., Srinivas, K., Pradeep, P., & Sarangapania, M. (2012). Synthesis, characterization and anti-microbial activity of new series of benzoxazole derivatives. *Int. J. Chem. Sci.* 10, 619–626.
2. Sana, T., & Sharad, W. (2012). Synthesis through microwave irradiation, characterization and evaluation of antimicrobial activity of 2-phenyl-l, 3 benzoxazole derivatives. *Int. Res. J. Pharm.* 3, 213–217.
3. Yamazaki, K., Kaneko, Y., Suwa, K., Ebara, S., Nakazawa, K., & Yasuno, K. (2005). Synthesis of potent and selective inhibitors of Candida albicans N-myristoyltransferase based on the benzothiazole structure. *Bioorg. Med. Chem.* 13, 2509–2522.
4. Koyama, E., Yang, G., & Hiratani, K. (2000). A novel synthesis of bis(benzoxazole) derivatives via tandem Claisen rearrangement. *Tetrahedron Lett*. 41, 8111–8116.
5. Krawiecka, M., et al. (2013). "Synthesis and biological activity of novel series of 1, 3-benzoxazol-2 (3H)-one derivatives." *Acta Pol Pharm*, 70.2, 245-53.
6. Ashurov, J., Karimova, G., Mukhamedov, N., Parpiev, N. A., & Ibragimov, B. (2011). Tetraaquabis [2-(2-oxo-2, 3-dihydro-1, 3-benzoxazol-3-yl) acetato] zinc. *Acta Crystallographica Section E: Structure Reports Online*, 67(4), m432-m432.
7. Ashurov, J. M., Mukhamedov, N. S., Tashkhodzhaev, B., & Ibragimov, B. T. (2015). Crystal structure of α-(N-benzoxazoline-2-one) acetic acid hydrate, solvate, and salts. *J. Struct. Chem.* 56(6), 1148-1153.
8. Wang, A., Ashurov, J.M., Ibragimov, A.B., Wang, R., Mouhib, H., Mukhamedov, N., & Englert, U. (n.d.). Charge density of the biologically active molecule (2-oxo-1,3-benzoxazol-3(2H)-yl)acetic acid. *J. Struct. Chem*, DOI: 10.1134/S0022476615060190
9. Ashurova, J. M., Izotovaa, L. Yu., Ibragimova, B. T., & Mukhamedovb, N. S. (n.d.). Two crystalline olymorphic forms of α-(n-benzoxazolin-2-one)acetic acid. Russ. *J. Phys. Chem.* DOI:10.1134/S0036024417010046
10. Wang, A., Ashurov, J.M., Ibragimov, A.B., Wang, R., Mouhib, H., Mukhamedov, N., & Englert, U. (2016). Charge density of the biologically active molecule (2-oxo-1,3-benzoxazol-3(2*H*)-yl)acetic acid. *Acta Cryst.* B72, 142–150. DOI:10.1107/S2052520615023690
11. Neese, F. (2012). ORCA Program system. *Comput. Mol. Sci.*, 2, 73-78.
12. Hanwell, M.D., Curtis, D.E., Lonie, D.C., Vandermeersch, T., Zurek, E., & Hutchison, G.R. (2012). Avogadro: An Advanced Semantic Chemical Editor, Visualization, and Analysis Platform. *J. Cheminf*, 4, 17.
13. Lu, T., & Chen, F. (2012). Multiwfn: A multifunctional wavefunction analyzer. *J. Comput. Chem*, 33, 580.
14. Humphrey, W., Dalke, A., & Schulten, K. (1996). VMD: Visual Molecular Dynamics. *J. Molec. Graph.*, 14, 33.
15. Banavath, H.N., Sharma, O.P., Kumar, M.S., & Baskaran, R. (2014, Nov.10). Identification of novel tyrosine kinase inhibitors for drug resistant T315I mutant BCR-ABL: a virtual screening and molecular dynamics simulations study. *Sci Rep*. 2014;4:6948. Published. doi:10.1038/srep06948
16. Kim, T., et al. (2020). Influence of ligand's directional configuration, chrysenes as model compounds, on the binding activity with aryl hydrocarbon receptor. *Sci Rep* 10, 13821 (2020). https://doi.org/10.1038/s41598-020-70704-9
17. Garza, J., Vargas R., Aquino N., Aquino N., Sen K.D. (2005). DFT reactivity indices in confined many-electron atoms. *J. Chem. Sci.*, Vol. 117(5), pp.379–386. https://doi.org/10.1007/BF02708341
18. Domingo, L.R., Ríos-Gutiérrez, M., & Pérez, P. (2016). Applications of the Conceptual Density Functional Theory Indices to Organic Chemistry Reactivity. *Molecules*, 21, 748; doi:10.3390/molecules21060748
19. Murray, J., & Politzer, P. (2011). The electrostatic potential: an overview. *WIREs Comput Mol Sci*. 1:153.
20. Johnson, E. R., Keinan, S., Mori-Sánchez, P., Contreras-García, J., Cohen, A. J., & Yang, W. (2010). Revealing Noncovalent Interactions. *Journal of the American Chemical Society, 132(18), 6498–6506.* doi:10.1021/ja100936w
21. Tan, S. L., Jotani, M.M., & Tiekink, E. R. T. (2019). Utilizing Hirshfeld surface calculations, non-covalent interaction (NCI) plots and the calculation of interaction energies in the analysis of molecular packing. *Acta Cryst*. E75, 308–318. https://doi.org/10.1107/S2056989019001129
22. Laplaza, R., et al. (2021). NCIPLOT and the analysis of noncovalent interactions using the reduced density gradient. WIREs Computational Molecular Science, 11 (2), pp.e1497. ff10.1002/wcms.1497ff. ffhal-02921299f
23. Şahin Akdeniz, E., & Selçuki, C. (2022). Investigation of interactions of doxorubicin with purine nucleobases by molecular modeling. *J.Mol.Model.*, Vol.28, 69. https://doi.org/10.1007/s00894-022-05031-z